The International Journal of Engineering and Science (IJES)
|| Volume || 7 || Issue || 6 Ver. II || Pages || PP 16-26 || 2018 ||
ISSN (e): 2319 – 1813 ISSN (p): 23-19 – 1805

Numerical Investigation of the Effects of Intake Port Geometry on In-Cylinder Motion and Combustion in Diesel Engine

Mahmut KAPLAN[1], Mustafa ÖZBEY[2,*] And Hakan ÖZCAN[2]
[1]*Amasya University, Faculty of Technology, Mechanical Engineering Department, Amasya, Turkey*
[2]*Ondokuz Mayıs University Engineering Faculty, Mechanical Engineering Department, Samsun, Turkey*
Corresponding Author: Mahmut Kaplan

----------*ABSTRACT*----------
Increasing pre-combustion turbulence level by air motion inside the intake system and combustion chamber is one of the significant elements to improve the fuel economyindiesel engines. In this study, different intake port configurationswere produced by rotating the base intake port about the cylinder axisand inclining it about the symmetry axis both 30° CW and CCW directions. The effects of these configurations on enhancingswirl, tumble, turbulence level and combustion efficiencywere numerically investigated during intake, compression,and power strokes by using RNG k-ε turbulent model in ANSYS FLUENT. The simulation results showed that the inclined port configurations such as -30I and +30I enhanced swirl ratio and created more turbulencenear TDC on the compression stroke comparing to other configurations. Therefore, -30I and +30I configurations augmented maximum pressure by 2.1 and 3.5% and increased the indicated fuel conversion efficiency by 2.5 and 3% compared to the base port. On the other hand, the rotatedport configurations such as -30R and +30Rdid not show a significant effect to improve swirl, tumble and turbulent kinetic energy. As a result, -30R configuration increased the indicated fuel conversion efficiency by 1.1 and +30R configurationdecreased the indicated fuel conversion efficiency by 1.4.
KEYWORDS: *Diesel engines, intake port, swirl, tumble, turbulence, combustion, CFD*

Date of Submission: 06-06-2018 Date of acceptance: 21-06-2018

I. INTRODUCTION

In CI (compression ignition) engine,the fuel injected into the cylinder is ignited by high-temperature air produced during the compression stroke. Therefore, rapid vaporization and proper air-fuelmixingare very important for burning of the injected diesel fuel completely. Moreover, due to strict environmental regulations,reducing exhaust emission in these engines must be necessary.One way to enhance combustion efficiency and reduce pollutant emission is generating in-cylinder flows such as swirl, tumble and squish by modifying the geometry of intake system and combustion chamber and placing flow blockages in the intake port. Swirl and tumble are both rotational flows whose axes parallel to piston motion and orthogonal to the cylinder axis, respectively. On the other hand, squish is a radial flow towards the center of the cylinder. Squish flow isobtained bysqueezing air between the piston and the cylinder head when the piston approachingTDC (top dead center) on the compression. The squishgenerates a secondary rotational flow called tumblearound a circumferential axis near the outer peripheral edge of the piston cavity. Turbulence in a cylinder is high during the suctionstroke but then reduces on the grounds thatair motion slows down near BDC (bottom dead center). It rises again during the compression due tothe intensification of swirl, tumble, and squish near the top dead center (TDC). At the end of the compression stroke, this large scale of organized flows breaks down into small-scale eddies which elevateturbulent intensity [1]. Thus, the more homogeneous air-fuel mixture isproduced before ignition and combustion efficiency is improved.

Recently, many researchers have examined numerically effects of organized rotational flows generatedby combustion chamber and intake system on enhancing turbulencelevel and fuel efficiency [2-9]. Payri et al.[2] evaluated the influence of different piston cavityshapes of a DI diesel engine on the in-cylinder motion characteristics throughthe suction and compression strokes by using CFD (computational fluid dynamics)calculations. It was concluded that during the suction stroke and the first half of the compression stroke, the piston configurations had little impact on the flow field whereas the piston-bowl shapesmade a notable contribution to the flow close to TDC and in the early part of the expansion stroke. Raj et al. [4] studied four piston geometries such as flat, inclined, flat center bowl and inclined offset bowl pistons in CI engine using STAR-CD CFD code and compared the simulation results of the piston configurations with experimental data obtained PIV (particle image velocimetry). The results showed that the simulated and experimental velocity profiles have similar flow pattern for all the piston shapes and a center bowl on the flat piston was a better configuration to enhance tumble flowand turbulence characteristics compared to other configurations.

Taghavifar et al. [6] analyzed the impact of modifying the shape of piston cavityas regardsincreasing the cavity distance from the center of the cylinder and the cavity radius by 2, 3 and 4times without changingCR (compression ratio) on the flow, burning performance and emission in a DI (direct injection) diesel engine. They summarized that on account of rising the cavity distance, the diesel fuel was more homogeneously mixed with air expense of the combustion beginning towards late expansion stroke, whereas elevating the cavity radius decreasedthemixture homogeneity because of these configurations diminishing rotational air motion in the combustion chamber. Furthermore, Harshavardhan et al. [7] used STAR-CD software to investigate in-cylinder flow parameters and interaction between intake flow and injected fuel spray of DIspark ignition engine with four different piston geometries. Their results were similarto Raj et al [4] thatat the beginning of injection, hightumble ratio and turbulent kinetic energy were obtained with the flat center bowl pistonin comparison to other piston configurations.On the other hand, Choi et al. [8] examined the effect of modified jet passage geometry in a swirl chamber type diesel engine on features of turbulence propertiesduring intake and compression strokes using VECTIS CFD code. They reported that decreasing the passage hole area of the swirl chamber led toa linear rise in the swirl.The large passage hole inclination of 40° produced the highest swirl and turbulent kinetic energy at the end of the compression process because of this configuration nearest to the direction of the piston motion.Bari et al. [9] proposed four guide vanesplaced in front of intake port with varied vane height such as R (intake runner radius), 0.25R, 0.50R and 0.75R to produce organized motions in the cylinderof a CI engine fueled with biodiesel. They examined impacts of these guide vaneson turbulence kinetic energy and engine performance by using SOLIDWORKS and ANSYS-CFX. Their study demonstrated that since 0.25R guide vane generated more turbulence, this vane helped to broke biodiesel fuel into smaller droplets causing well mixing of air and so enhanced combustion.

The aim of this study is to investigate different intake port configurations which induce rotational flows in the cylinder of a DI diesel engine andto evaluate the influences of these configurations on turbulence and combustion parameters by using ANSYS WORKBENCHplatform.

II. COMPUTATIONAL METHODS

2.1 The steps of the numerical simulation process

Two methods such as hybrid and layering approaches are generally used to deal with in-cylinder flow analysis in ANSYS FLUENT. The hybrid method is mainly employed for spark ignited engines (SI)with canted valve, whereas the layering method is mostly appliedtodiesel engines with vertical valves. In this study, layering approach was used in the simulation of a DI diesel engine. The technical specifications of the engine are presented in Table 1.

Table 1 The engine specifications

Type	Single cylinder, four-stroke CI engine
Bore	87.5 mm
Stroke	110 mm
Connecting rod length	234 mm
Valve diameter	34 mm
Piston cavity	Hemispherical (diameter 51.5 mm)
Engine speed (N)	1500 rpm
Compression ratio	17.5
Intake valve opening	355.5º (4.5º BTDC, exhaust stroke)
Intake valve closing	575.5º (35.5º ABDC, compression stroke)
Exhaust valve opening	144.5º (35.5 º BBDC, power stroke)
Exhaust valve closing	364.5º (4.5º ATDC, intake stroke)
Number of orifice x diameter	3 x 0.24 mm
Separation angle of orifice	120º
Injection spray angle	60º (the cylinder axis.)
Fuel injection pressure	200 bar
Fuel injection timing and duration	697º (23º BTDC, compression stroke), 29º
Fuel	$C_{14,6}H_{24,8}$(heavy diesel)
Cetane number	49
Injected fuel and fuel flow rate	0.0293 g/cycle, 0.0091 kg/s

The parts of geometry including the piston bowl, the cylinder, the intake and exhaust valves,and portswere produced and assembled using SOLIDWORKS. Then, the constructed geometric model was decomposed and meshed with suitable mesh methods using ANSYS WORKBENCH platform as shown inFig. 1.

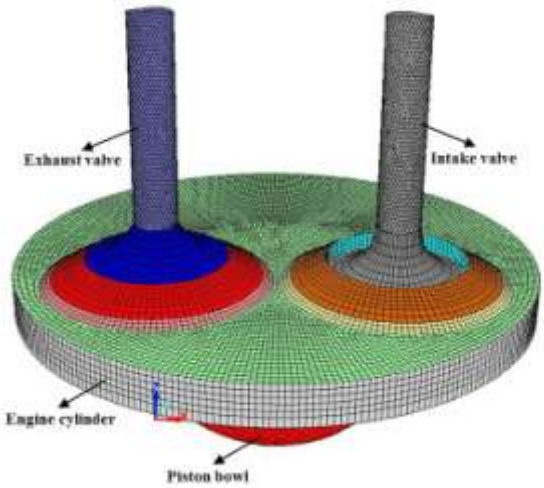

Fig. 1. Different zones in the geometry

In this step, owing to the model breaking up into different zones, various mesh motion techniques were implemented todistinct regions in a single simulation. After this,models, boundary conditions and the necessary motion for valves and piston were defined in ANSYS FLUENT. Finally, numerical computations and post-processing of the simulation results were performed. In this work, the CFD analysis was accomplishedduring the intake, compression and expansion strokes.

2.2 Configurations

The fourpossible intake port geometrieswith same CRwere produced by rotating and inclining of the base intake port. Since the modelled intake and exhaust ports are very close to each other, all configurations were generated after the exhaust port moved forward to its new positionas shown in Fig. 2.

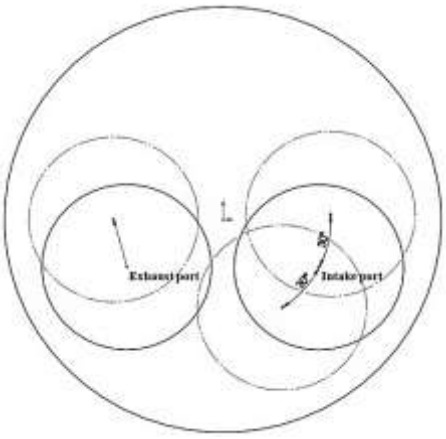

Fig. 2. Rotation of the base intake port around the cylinder axis

-30R and +30R configurations were obtained by 30° CCW (counter clockwise) and CW (clockwise) rotation of the baseintake port around the cylinder axis as illustrated in Fig. 3 (a) and (b) respectively. On the other hand, -30I and +30I configurations were generated by the inclination of the base intake port CCW and CW direction around the symmetry axis of thebase port as illustrated in Fig.3 (c) and (d), respectively.

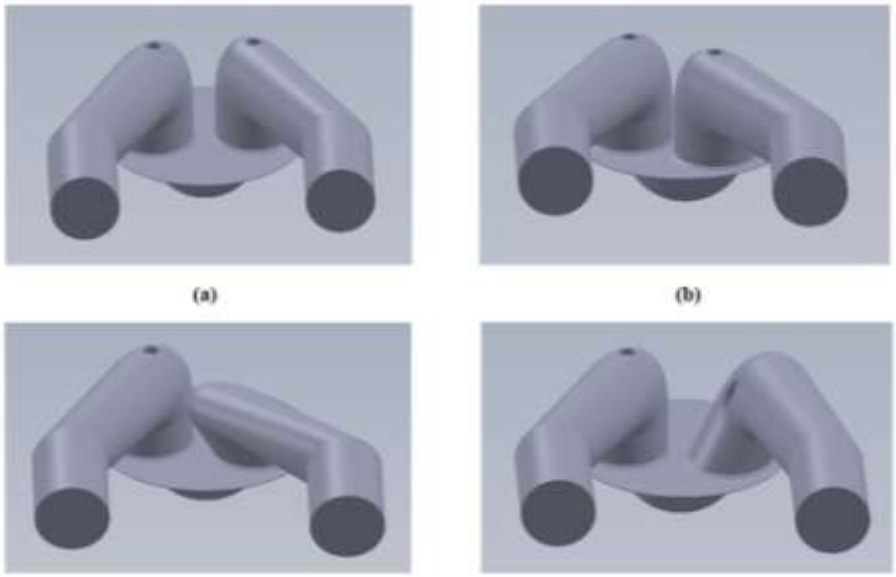

Fig.3.The various intake port configurations:a) -30R b) +30R c) -30I d) +30I (R and I are rotation and inclination respectively)

2.3 The turbulence model

RNG k-ε turbulence modelwas employedfor predicting turbulent flow in the cylinder of DI diesel engine. RNG k-ε model contains the extra termin the dissipation equation.Thus, RNG model moreaccurately identifies flows with regions of intense strainrate. The influence of swirl flow on turbulence is also considered in this modelto envisage swirling flowscorrectly.The transport equation for the turbulent kinetic energy *k* and the turbulence dissipation rate *ε*are[10].

$$\frac{\partial}{\partial t}(\rho k)+\frac{\partial}{\partial x_i}(\rho k u_i)=\frac{\partial}{\partial x_j}\left[\alpha_k \mu_{eff}\frac{\partial k}{\partial x_j}\right]+G_k+G_b-\rho\varepsilon-Y_M+S_k \quad \textbf{(1)}$$

$$\frac{\partial}{\partial t}(\rho\varepsilon)+\frac{\partial}{\partial x_i}(\rho\varepsilon u_i)=\frac{\partial}{\partial x_j}\left[\alpha_\varepsilon \mu_{eff}\frac{\partial \varepsilon}{\partial x_j}\right]+C_{1e}\frac{\varepsilon}{k}(G_k+C_{3e}G_b)-C_{2e}\rho\frac{\varepsilon^2}{k}-\frac{C_\mu\rho\eta^3(1-\eta/\eta_0)}{1+\beta\eta^3}\frac{\varepsilon^2}{k}+S_\varepsilon \quad \textbf{(2)}$$

where$\rho$is the fluid density, $x_i$and x_j are Cartesian coordinate, $u_i$is absolute velocity component in direction x_i.μandμ_t are the dynamic and the turbulent eddy viscositycoefficients, respectively. The production of turbulence kinetic energy owing to the mean velocity gradients and buoyancy are calculated by $G_k$and G_b. $Y_M$is the contribution of the fluctuating dilatation incompressible turbulence to the overall dissipation rate. $S_k$and $S_\varepsilon$are the user determined source terms.$C_{1\varepsilon}$, $C_{2\varepsilon}$,and $C_\mu$are constants whose values are 1.42, 1.68and 0.0845in this work, respectively.

2.4Calculation of SR, TR,and TKE

A dimensionless parameter known as the swirl ratio is used to quantify the swirl motion within the cylinder. The swirl ratio is obtained as [11].

$$SR=\frac{\omega_s}{(2\pi N/60)} \quad \textbf{(3)}$$

where*SR* swirl ratio, $\omega_s$is swirl angular speed, rad/s, *N* is engine speed, rpm.A tumble ratio is also a dimensionless parameter used to characterize the magnitude of tumble flow expressedas

$$TR = \frac{\omega_t}{\left(2\pi N/60\right)} \textbf{(4)}$$

where *TR* is tumble ratio, $\omega_t$is tumble angular speed, rad/s.The turbulent kinetic energy, *k*is described asthe average fluctuating kinetic energy per unit masswith unit m^2/s^2 in a turbulent flow.*k* is calculated by

$$k = \frac{1}{2}\left(u_x^{'2} + u_y^{'2} + u_z^{'2}\right) \textbf{(5)}$$

where$u_x^{'2}$, $u_y^{'2}$and$u_z^{'2}$arethe turbulent fluctuation velocities relating to flow directions*x*, *y* and *z* respectively.

2.5 Combustion model

The combustion process in the diesel engine was modelled by the species transport model combined with the eddy dissipation. In this approach, the local mass fraction of each species was predicted through the solution of convection-diffusion equation for the *i*th species. The transport equation for the *i*th species is as follows [10]

$$\frac{\partial}{\partial t}(\rho Y_i) + \nabla(\rho v Y_i) = R_i + S_i - \nabla J_i \textbf{(6)}$$

where Y_i is a local mass fraction of each species, R_i, the net rate of generation of species *i* due to chemical reaction, is calculated by the eddy-dissipation model founded on the work of Magnussen and Hjertager [12]. S_i is the rate of creation by addition from the dispersed phase and any user-defined source. J_i is the diffusion flux for turbulent flows calculated as

$$J_i = -\left(\rho D_{i,m} + \frac{\mu_t}{Sc_t}\right)\nabla Y_i - D_{T,i}\frac{\nabla T}{T} \textbf{(7)}$$

where $D_{i,m}$is the diffusion coefficient of the *i*th species in the mixture, $\mu_t$is the turbulent dynamic viscosity and Sc_t is the turbulent Schmidt number which is equal to 0.7 by default. $D_{T,i}$is the turbulent diffusivity and∇T is the temperature gradient. The ignition delay period was predicted by using the Hardenburg and Hase ignition delay modelfor diesel engines[13].

2.6Spray model

Solid-cone injector model was chosen to represent the primaryspray break-up. Solid-cone atomizer gives initial particle conditions in terms of appropriate nozzle parameters such as spray angle and nozzle diameter.The Kelvin-Helmholtz-Rayleigh-Taylor (KH-RT) model was used to describe secondary breakup [10].In this study, the drop size constant B0 and the breakup time constant B1 were taken to be0.61 and 24, respectively, for all simulations.Droplet collision and coalescence weredealt with by O'Rourke's model [14].

2.7 Boundary conditions

Intake and exhaust ports pressure were held constant. Thus, the dynamic effects were disregarded during the simulation of these regions. The initial pressure and temperature at the inlet and outlet boundaries were 1 atmospheric and 300 K, respectively. Both variables regarded as homogeneous in the complete domain. The engines walls were described as stationary withthe no-slipcondition. The fixed temperature was specified as a thermal boundary condition at walls. The temperature of intake and exhaust ports are 300 K and temperature of the cylinder head, cylinder wall and piston are 400 K. The flow was supposed fully developed. The turbulence intensity at the core of fully-developed duct flow can be estimated using following empirical correlation for pipe flows:

$$I = 0.16\left(Re_{d_h}\right)^{-1/8} \textbf{(8)}$$

where $Re_{d_h}$is the Reynolds number calculated according to the pipe hydraulic diameter,d_h. In this simulation, turbulence intensity of 5% and hydraulic diameter of 0.03 m wereemployed forturbulence model parameters at the inlet and outlet.

III. RESULTS AND DISCUSSION

3.1 Grid independence test and validation

Prior to performing the CFD simulation of the diesel engine, the grid independence testwasconductedtoestablish the optimum grid size. Two grids having 378423 and 730734 cells were compared with experimental results of Jaichandar et al. [15] in Fig. 4. In the grid size of 730734 cells, CFD predictions of the pressure gradient over the combustion period and the peak pressure was in a reasonably good agreement with the experimental data compared to the grid size of 378423. Hence, this grid was considered in the following simulation studies.

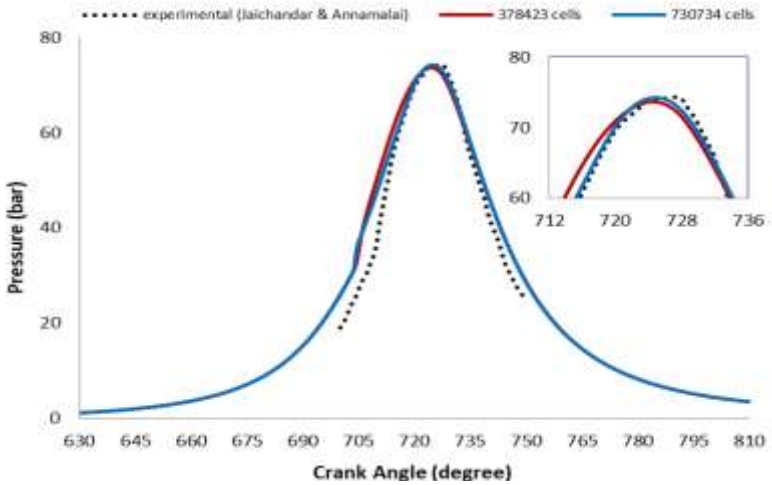

Fig. 4. Comparison of computational and experimental results for in-cylinder pressure

3.2Average swirl flow in the cylinder

Fig.5demonstrates the changeof swirl ratio in the cylinder according to crank angle during the intake, compression and power strokes for various intake port configurations.As can be seen in Fig. 5, there is an increase of swirl ratio during the early stage of the suction for all intake port configurations but for +30º CW inclined port in which the direction of the swirl is negative. The increase of the swirl in this stage is expected because of the piston acceleration and reduction of pressure inside the cylinder. The first peak occurs at beginning of the second part of the intake stroke. After reaching the first peak, the swirl starts decreasing owing to the increase in the volume of the cylinder, reduction of mass flow rate of incoming air by a closing intake valve and dissipation of angular momentum due to the friction between the wall and air inside the cylinder. However, the swirl ratio persistsnearly constant during the early stage of the compression stroke. Then the swirl ratio again rises during the late compression stroke because of the tangential velocity of the swirling flow enhanced due to the interaction between the piston cavity and combustion chamber. This trend of the swirl ratio was found earlier by Payri [2] and Micklow et al. [16].According to Fig. 5, the inclined base port configurations such as -30I and +30I generate the maximum positive and negative swirl ratios of 5.19 and -5.40 respectively at the end of the compression stroke when the maximum swirl ratio of the base intake port is 1.17. This was probably on account of the inclined intake port configurations which augment tangential velocity during the intake stroke. On the other hand, configurations produced by rotating intake port such as -30R and +30R are not effective to increase the swirl ratio. Therefore, -30R and +30R configurations have the maximum swirl ratios of 1.53 and 0.63 respectively.

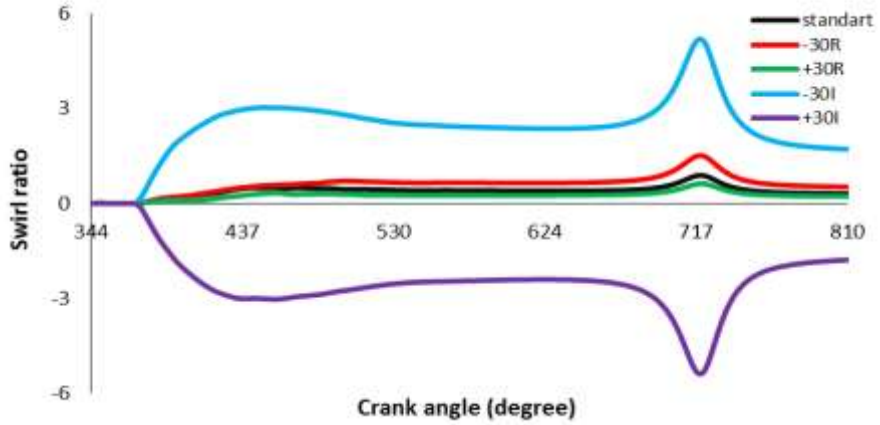

Fig. 5.Swirl ratio variations versus crank angle for different configurations

3.3Average tumble flowin the cylinder

In general, tumble motion divides into four distinct phases such as tumble generation, stabilization, spin-up and decay [17]. The tumble generation phase lasts during intake process from TDC to BDC(between 360° and 540°) in Fig.6.As shown in the figure, the tumble ratio about x and y-axes(tumble ratio-x and tumble ratio-y) increasefor all configurations because of the intake flow interacting with cylinder wall and moving piston towards BDC in this phase.+30R and -30I configurations considerably improvethe tumble ratio-x of 1.14 and 1.08comparedto the base port having tumble ratio-x of 0.49 in Fig. 6 (a).

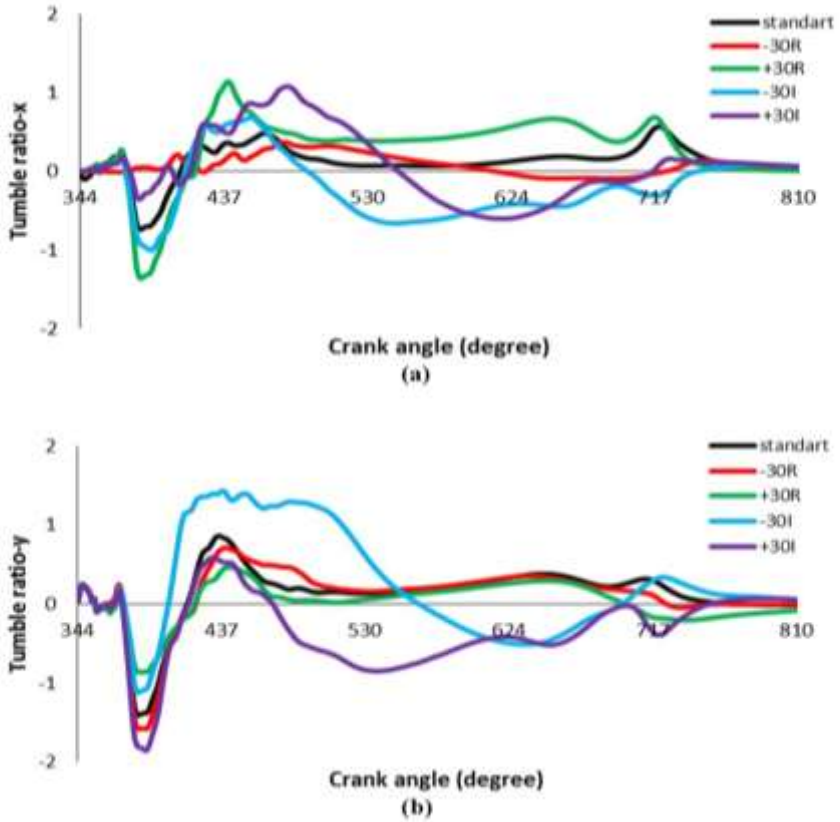

Fig. 6. Tumble ratio variations versus crank angle for different configurations: a) tumble ratio about x-axis, b) tumble ratio about y-axis

On the other hand, the highest tumble ratio-y of 1.42 is obtained by -30I configuration when compared to the base port having tumble ratio of 0.86 in Fig. 6 (b). Then tumble stabilization phase occurs between intake BDC(540°) and the closing of the intake valve (575.5°)and tumbleratio decreases considerably end of this phase due to friction at the cylinder wall and the upward movement of the piston as shown Fig. 6. After this, in the

tumble spin-up phase, tumble ratio increases again due to compression of in-cylinder flow by the upward-moving piston and then a decrease of tumble ratio gradually extends at end of the compression stroke (720°) in tumble decay phase.

3.4Average turbulent kinetic energyin the cylinder

The turbulent kinetic energy in the combustion chamber at the end of the compression process is one of the significant factors that affect the mixture of the fuel and air and the regulation of combustion process along with the fuel spray characteristics in diesel engines. Fig. 7 illustratesa comparison of the turbulent kinetic energy withdifferent configurations during intake, compression and power strokes. It is observed that the configurations follow the same trend. The behavior of the turbulence characteristics may be identified three stages such as intake produced turbulence, swirl-tumble augmented turbulence,and decay. The first phase continues between the intake TDC and the beginning of the compression. In this phase, the intake flow is a major source of turbulence. The turbulent kinetic energy reaches a peak valuerelying on intake port and valve shapeand flows conditions in the combustion chamber. Then it decreases in the decay phase.

As shown in Fig.7, the highest turbulent kinetic energy of 44.7 m^2/s^2 is obtained by -30I configuration and it isapproximately 22.1% higher compared with the base model. This result is predictedsince -30I port configuration significantly improves both swirl and tumble ratios during intake stroke as shown in Figs. 5 and 6. On the other hand, +30R and +30I configurations increase the maximum value of turbulent kinetic energy of 1.7 and 2.1% by respectively whereas -30R configuration reducesthe maximumturbulent kinetic energy by 3.9%. The second phase extends from the end of the first phase to a point where turbulent kinetic energy reaches the second peak. In this stage, the organized flows such as swirl and tumble breakdown mainly attribute to enhance turbulence. As could be seen fromFig.7, -30I and +30I configurations play an important role in generating the turbulence inside the combustion chamber comparing the base portand these configurations increase the turbulent kinetic energy noticeably during injection (between 697° and 726°). For instance, at 711° (9° before TDC in compression stroke) -30I and +30I configurations produce the turbulent kinetic energy of 7.3 and 7.1 $m^2/s^2$and theyare16 and 13% higher than the base intake port generated the turbulent kinetic energy of 6.3 m^2/s^2. It is concluded that -30I and +30I configurationsincreased swirl and tumble ratios and this results in augmentation of the turbulent kinetic energy near the TDC of the compression stroke.

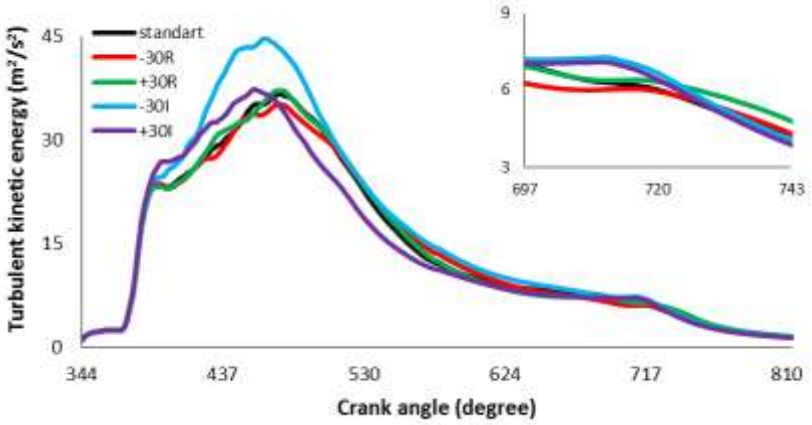

Fig. 7. Turbulent kinetic energy variations versus crank angle for different configurations

3.5 Average pressure in the cylinder

The results of in-cylinder pressure for different configurations are illustrated in Fig.8. As shown in the Fig. 8, -30I and +30Iintake port configurations have higher in-cylinder pressure than the other configurations. Higher peak pressure using the inclined port configurations is anticipated as a result of these configurations produced higher swirl, tumble and turbulent kinetic energy during intake and compression strokes.The maximum pressure values of 75.8 and 76.9 bar are obtained by -30Iand +30Iconfigurations when compared to the base port having a value of 74.1 bar.Therefore, these configurations elevatethe maximum pressure of 2.1 and 3.5% compared to the base port. On the other hand, since -30R and +30R configurations do not contribute significantly to the increaseof the turbulence and the maximum pressure, these configurationsreduceby 1.1 and 0.2%compared to the base configuration as shown in Fig. 8.

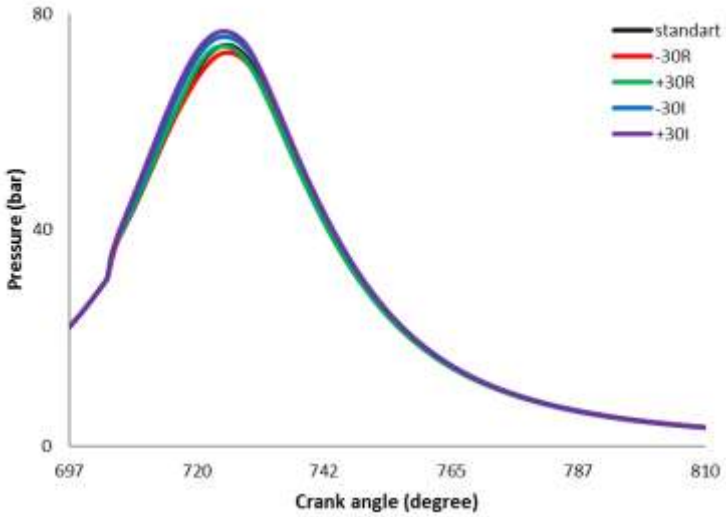

Fig. 8. Pressure variations versus crank angle for different configurations

3.6Average temperature and heat release rate in the cylinder

As shown in Fig. 9, -30I and +30I configurations increase temperatures of the combustion chambers near TDC in the compression stroke and this trend continues towards the expansion stroke like in-cylinder pressure in Fig. 8. Therefore,-30I and +30I configurations improve maximum in-cylinder temperature of 1717 and 1741 K and increase by 4.3 and 5.8% when compared to the base port having temperature of 1646 K.However, the configurations produced by rotating the base portare not so effective in increasing the temperature of the chamber similar to the pressure in Fig. 8.Hence,+30R configuration reducesthe temperature of 1633 K by 0.8% compared to the base configuration.

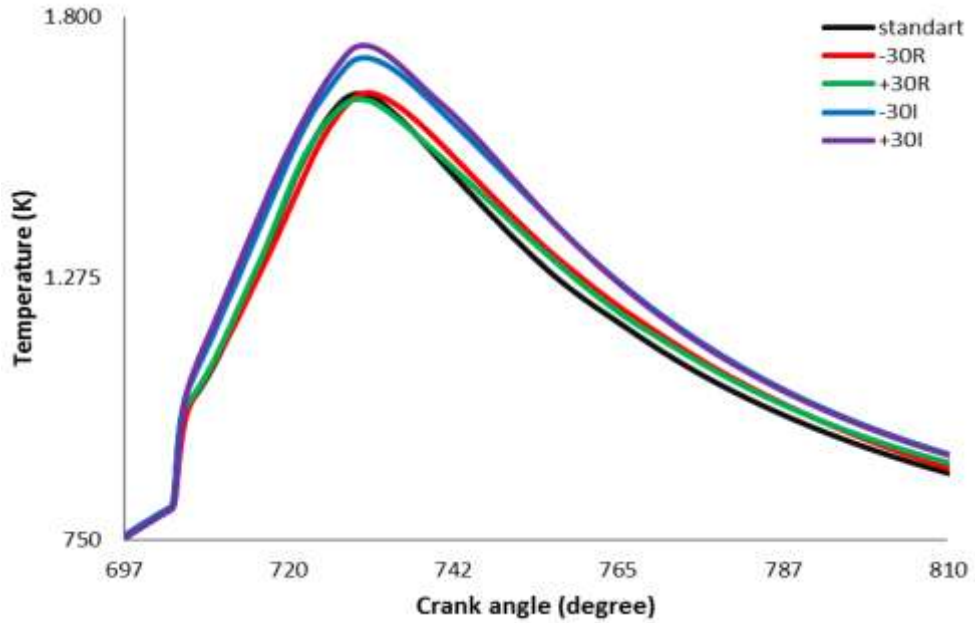

Fig. 9. Temperature variations versus crank angle for different configurations

As seen in Fig.10, since increasingturbulent levelat the end of the compression stroke in Fig. 7 improves air-fuel mixing, -30I and +30I configurations enhanced heat release rate at the end of the compression stroke (720°)when compared the base port.

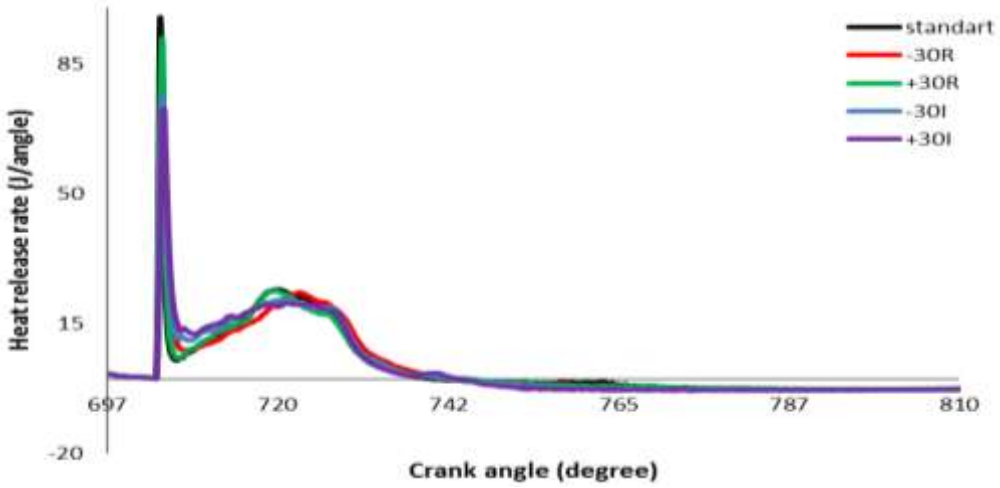

Fig. 10. Heat release rate variations versus crank angle for different configurations

3.7 Average indicated fuel conversion efficiency in the cylinder

The indicated fuel conversion efficiency, $\eta_{f,i}$is the ratio of work generated per cycle to the amount of fuel energy supplied (1). $\eta_{f,i}$is calculated as

$$\eta_{f,i} = \frac{W_i}{m_f Q_{LHV}} \textbf{ (9)}$$

where W_i is the indicated work per cycle and it is the sum of the compression stroke work andthe expansion stroke work:

$$W_i = W_C + W_E \textbf{ (10)}$$

where W_C and $W_E$are the compression stroke work and the expansion stroke work respectively. $Q_{LHV}$is the lower heating value of the fuel. In this study, $W_i$is calculated using MATLAB.As can be seen in Fig.11, since the intensification of turbulent kinetic energy with the organized flows, improve W_E which is positive work, -30I and 30I configurations increase the indicated fuel conversion efficiency of 2.5 and 3% respectively when compared to the base port. On the other hand, despite decreasing maximum pressure with -30R configuration, the indicated fuel conversion efficiency increases 1.1%by this configuration. This may be due to an increase of swirl by -30R configuration in Fig. 5 improving the indicated work in the expansion stroke.However,since +30R configurations do not improve swirl ratio in Fig. 5, it is ineffective to elevatethe indicated fuel conversion efficiency and this configurationdecrease the indicated fuel conversion efficiency by 1.4%.

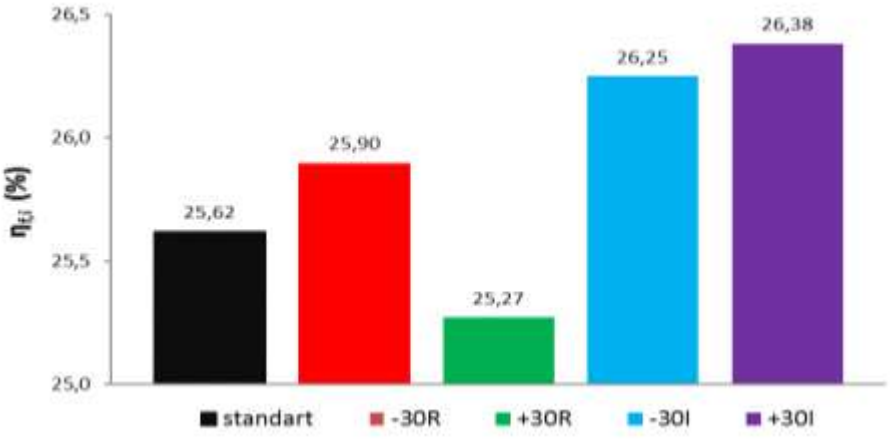

Fig. 11. The indicated fuel conversion efficiency variations versus crank angle for different configurations

IV. CONCLUSIONS

In this research, the impacts of various intake port configurations on in-cylinder flow, turbulence intensity and diesel fuel performancehave been examined numerically for RNGk-ε turbulent model during intake, compression and power strokes using ANSYS FLUENT code. The following results were concluded.

1. Variation of swirl ratio followsthe same trend during simulation withconfigurations obtained by rotation and inclination of the straight intake port. Having higher tumble and swirl ratios, the inclined intake port configurations such as -30I and +30Iincrease turbulent kinetic energy during the intake stroke. -30I configuration produces the maximum turbulent kinetic energy of 44.7 m^2/s^2 compared the other configurations. In compression stroke, -30I and +30I configurations also generates the maximum positive and negative swirl ratios of 5.19 and -5.40respectively. Therefore, these configurations increased the turbulent kinetic energy during the injection.
2. -30I and +30I configurations contribute to enhancing air-fuel mixing resulting inimproving maximum pressure and fuel conversion efficiency. Thus, -30I and 30I configurationselevatethe maximum pressure 2.1 and 3.5% and improve the indicated fuel conversion efficiency 2.5 and 3% respectively, compared to the base port.
3. On the other hand, configurations generatedby rotating the base port such as -30R and +30R do not have the beneficial effect of augmenting turbulent kinetic energy. But,despite decreasing maximum pressure,-30R configuration increase fuel conversion efficiency 1.1%.This may be due to increasing swirl ratio with -30R configuration improving positive work in expansion stroke when compared the base port.

REFERENCES

[1]. Heywood, J. B. (1988). Internal combustion engine fundamentals, McGraw-Hill, New York.
[2]. Payri, F., Benajes, J., Margot, X., and Gil, A. (2004). CFD modeling of the in-cylinder flow in direct-injection Diesel engines, Computers & Fluids, 33: 995-1021.
[3]. Rakopoulos C.D., Kosmadakis G.M., Pariotis E.G., 2010. Investigation of piston bowl geometry and speed effects in a motored HSDI diesel engine using a CFD against a quasi-dimensional model, Energy Conversion and Management, 51, 470-484.
[4]. Raj A. R. G. S., Mallikarjuna J. M. and Ganesan V. (2013.). Energy efficient piston configuration for effective air motion – A CFD study, Applied Energy, 102: 347-354.
[5]. Wei S., Wang F., Leng X., Liu X., Ji K., 2013. Numerical analysis on the effect of swirl ratios on swirl chamber combustion system of DI diesel engines, Energy Conversion and Management, 75, 184-190.
[6]. Taghavifar H., Khalilarya S., and Jafarmadar S. (2014). Engine structure modifications effect on the flow behavior, combustion, and performance characteristics of DI diesel engine, Energy Conversion and Management, 85: 20-32.
[7]. Harshavardhan B & Mallikarjuna J M (2015). Effect of piston shape on in-cylinder flows and air-fuel interaction in a direct injection spark ignition engine - a CFD analysis. Energy, 81, 361-372.
[8]. Choi G. H., Kim S. H., Kwon T. Y., Yun J. H., Chung Y. J., Ha C. U. , Lee J. S., Han S. B. (2006) A numerical study of the effects of swirl chamber passage hole geometry on the flow characteristics of a swirl chamber type diesel engine, Journal of Automobile Engineering, 220: 459-470.
[9]. Bari S. and Saad I., (2013). CFD modelling of the effect of guide vane swirl and tumble device to generate better in-cylinder air flow in a CI engine fuelled by biodiesel Computers & Fluids, 84: 262-269.
[10]. ANSYS FLUENT Theory Guide (Release 14.0, November 2011).
[11]. Pulkrabek, W-W. (1998). Engineering Fundamentals of the Internal Combustion Engine, Prentice-Hall, Upper Saddle River, New Jersey.
[12]. Magnussen B F & Hjertager B H (1976). On mathematical models of turbulent combustion with special emphasis on soot formation and combustion. 16th Symposium. (International) on Combustion, soot formation and growth, 719-729, the Combustion Institute Pittsburgh, PA.
[13]. Hardenburg H. O. and Hase F. W. An Empirical Formula for Computing the Pressure Rise Delay of a Fuel from its Cetane Number and from the Relevant Parameters of Direct Injection Diesel Engines. SAE Technical Paper 79049, (1979).
[14]. P.J. O'Rourke. Collective Drop Effects on Vaporizing Liquid Sprays. PhD thesis, Princeton University, Princeton, New Jersey, 1981.
[15]. Jaichandar S & Annamalai K (2012). Effects of open combustion chamber geometries on the performance of pongamia biodiesel in a DI diesel engine. Fuel, 98, 272-279.
[16]. Micklow, G.J., Gong W.D. (2007). Intake and in cylinder flow field modeling of a four valve diesel engine, Journal of Automobile Engineering, 221:1425-1440.
[17]. Achuth M., Metha P.S. (2001). Predictions of tumble and turbulence in four-valve pentroof spark ignition engines, International JDenklemi buraya yazın.ournal of Engine Research, 2: 209-227.

Mahmut Kaplan." Numerical Investigation of the Effects of Intake Port Geometry on In-Cylinder Motion and Combustion in Diesel Engine." The International Journal of Engineering and Science (IJES) 7.6 (2018): 16-26